In Silico Mixed Lubrication Model to Evaluate the Radial Clearance Influence on the Tribology of Total Hip Replacement

Alessandro Ruggiero[1(✉)] and Alessandro Sicilia[2]

[1] Department of Industrial Engineering, University of Salerno, Via Giovanni Paolo II, nº 132, 84084 Fisciano, Italy
ruggiero@unisa.it

[2] Department of Industrial Engineering, University of Salerno, Via Giovanni Paolo II, nº 132, 84084 Fisciano, Italy
asicilia@unisa.it

Abstract. In biomechanics and biotribology the attention of scientific community is actually paid to the tribological optimization of the design parameters of prosthetic implants, devoted to the substitution of an unhealthy synovial articulation: a tribological characterization of the artificial joint is needed in order to guarantee minimum wear and maximum duration.

The aim of this manuscript is to show the results about the development of a tribological model of the artificial hip joint made of Ultra High Molecular Weight PolyEthylene acetabular cup against ceramic femoral head: the model is supplied with the hip loading and relative motion coming from a multibody model developed by the authors in another work and it is used to analyze the response of several tribological quantities with respect to a variation of the implant radial clearance.

The algorithm, written in Matlab computational environment, is based on the Reynolds equation adapted to the mixed lubrication mode: the results provided expected trends in terms of fluid/contact pressure, surfaces' separation, wear penetration depth, etc. which could result in maps able to be used to find an optimal geometrical configuration of the implant dedicated to the framework of the customized subject-specific prostheses.

Keywords: Biotribology · Total Hip Replacement · Mixed Lubrication · In-silico

1 Introduction

The human synovial articulation is characterized by a cavity separating the linked bone extremities covered by cartilage; it is filled by the synovial fluid providing the lubrication to the joint and giving the maximum relative mobility with minimum friction by alternating complex full film and/or boundary lubrication mechanisms.

Because of aging or articular diseases the cartilage tends to deteriorate, so that a surgical procedure of replacement of the unhealthy articulation with an artificial implant

M. Okada (Ed.): IFToMM WC 2023, MMS 149, pp. 855–860, 2024.
https://doi.org/10.1007/978-3-031-45709-8_83

could be requested. The tribo-mechanical design of the artificial joint has to globally guarantee the minimum wear so that the number of the successive surgical revisions is minimized [1, 2].

The tribological analysis [3] could be conducted in silico by the physical and mathematical definition of the investigated phenomena and turning them in a numerical model. In particular, the mixed lubrication mode is necessary to be modeled due to experimental evidence referred to artificial hip joint during the gait [3]: several numerical approaches have been developed in this framework by studying the coexistence of lubricated and contact zones during the contact numerical simulation based on the Reynolds equation and the wear modelling in this context [4–6].

The objective of the authors is to show the structure of the algorithm developed in the framework of the same author's works [7–12], which is supplied by the hip load and relative motion associated to the gait kinematics elaborated by a multibody model [8] and it provides results about the time evolution of the fluid/contact pressure, the surfaces' separation, the eccentricity of the femoral head with respect to the acetabular cup and the cumulated wear volume. In particular the output will be analyzed with respect to a variation of the artificial joint radial clearance.

2 Materials and Methods

The model (Eq. (1)) is based on the Reynolds equation in which the unknown fluid pressure p and the contact pressure p_c are numerically calculated along the analyzed time t by knowing the synovial fluid rheological properties of density ρ and viscosity μ, the surface's separation h and the entraining velocity vector $\boldsymbol{v}$. The domain $\Omega\Omega$ is divided into lubricated zones where the surface's separation h is greater than a boundary thickness Δ_b and contact zones otherwise (the thickness Δ_b is included in order to avoid numerical instabilities in correspondence of the transition between lubricated and contact zones due to the nature of the Reynolds equation); the zero pressure is imposed on the domain boundaries $\partial\Omega$. The surface's separation h is composed by the geometrical approach defined by the eccentricity vector $\boldsymbol{e}$ projected along the radial direction $\hat{\boldsymbol{r}}$ and the radial clearance c, by the surface's deformation δ dependent on the fluid pressure p through the constrained column deformation model, the contact deformation elaborated by the same deformation model supplied by the contact pressure p_c and the wear penetration depth u_w evaluated through the Archard wear model. The entraining velocity vector $\boldsymbol{v}$ is composed by a translational contribution due to the time derivative of the eccentricity and by a rotational contribution due to the angular velocity vector $\boldsymbol{\omega}$ (R is the cup radius). All the analyzed implant parameters involved in the simulations are the same used in [7].

$$\begin{cases} h = c - \boldsymbol{e}^T\hat{\boldsymbol{r}} + \delta(p) + \delta(p_c) + u_w \\ \boldsymbol{v} = \dot{\boldsymbol{e}} + \boldsymbol{\omega} \times \left[(R-h)\hat{\boldsymbol{r}} - \boldsymbol{e}\right] \\ \nabla \cdot \left(\frac{\rho h^3}{12\mu}\nabla p\right) = \nabla \cdot (\rho h \boldsymbol{v}) + \frac{\partial}{\partial t}(\rho h) \quad if h \geq \Delta_b \\ \delta(p_c) = \Delta_b - \left(h_g + \delta(p) + u_w\right) \quad if h < \Delta_b \\ p = 0 \quad on \partial\Omega \end{cases} \tag{1}$$

The rheological properties of viscosity μ and density ρ are defined by their dependence on the fluid pressure p through the Dowson-Higginson model combined with the Cross non-Newtonian one and the Barus model, respectively, reported in the Eq. (2), in which the parameters k_μ and n_μ govern the viscosity variation within the range delimited by the viscosities μ_0 and μ_∞ (shear-thinning non-Newtonian behavior), the parameter α_μ regulates the viscosity exponential growth with respect to the pressure and the parameters a_ρ and b_ρ manage the density increase due to an increasing pressure.

$$\mu = \left[\mu_\infty + \frac{\mu_0 - \mu_\infty}{1 + k_\mu \left(\frac{v_{sl}}{h}\right)^{n_\mu}}\right] e^{\alpha_\mu p} \quad \rho = \rho_0 \frac{a_\rho + b_\rho p}{a_\rho + p} \tag{2}$$

The model represented by the governing Eqs. (1) and (2) is solved numerically, due to its high non-linearity through the finite differences method, for five linearly spaced values of radial clearance going from 50, μm to 150, μm; it is supplied by the gait hip loads and angular velocities coming from the multibody model developed in [8] and it is run iteratively so that the total pressure over the surfaces balances the hip loads. The schematic workflow is shown in the Fig. 1.

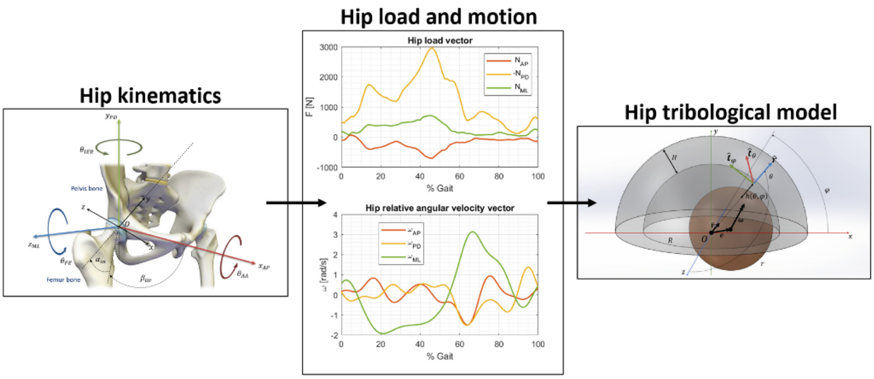

Fig. 1. Model schematic workflow

3 Results and Discussions

In the following, the results are summarily shown in the Fig. 2 in terms of surfaces varying with respect to the two spherical angles directions θ and φ [7] intersecting in correspondence of the pressure peak and to the radial clearance.

In particular, the total pressure and the surface separation profiles are reported during both a full film and a mixed phase.

A growing radial clearance, causing a lower geometrical conformity between the coupled surfaces, causes:

– an increasing fluid pressure peak and a decreasing minimum separation while their profile shapes progressively shrink, producing a more localized deformed area during the full film phase;

– an increasing contact pressure peak is retrieved and a decreasing contact area is visualized during the mixed phase.

Then, the wear volume cumulated at the end of the gait cycle, the maximum pressure reached in the synovial cavity and the maximum contact area fraction are reported in the bar graphs (the contact area fraction is defined as the percentage of direct contact area over the whole cup surface): as expected, since the maximum pressure grows with the increasing radial clearance, for the same relative motion the wear volume tends to grow, except for the 75 μm radial clearance (this behavior directly depends on the logic adopted by the algorithm to rule the contact occurring eventuality, so, even if a global wear volume increase is retrieved, this is subject of deepening for the authors); the presence of the latter outlier can be attributed to the stability of the contact occurring condition explained in the Eq. (1), which produces also a non-strictly decreasing maximum contact area fraction depicted in the bar graph reported in the Fig. 2.

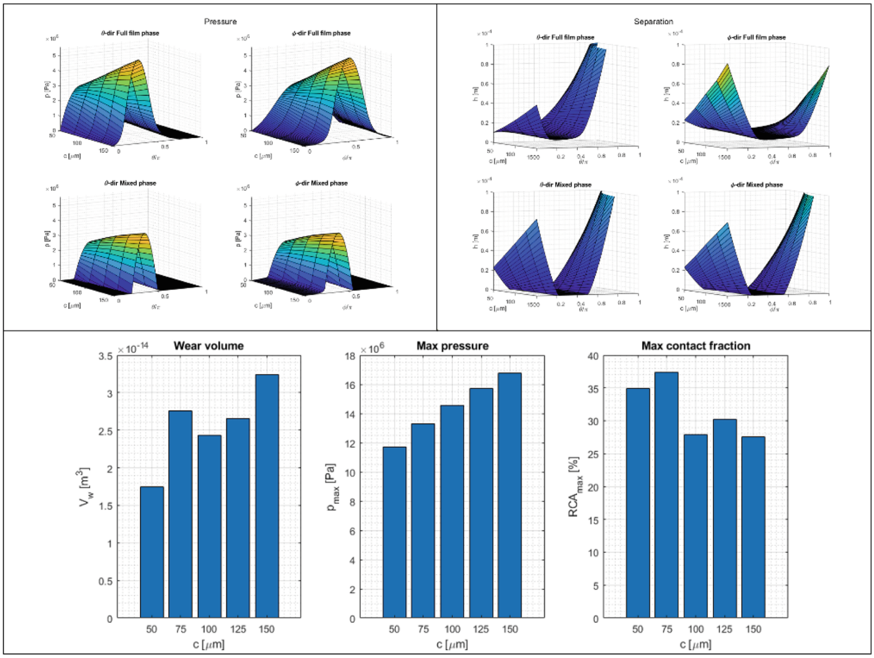

Fig. 2. Pressure, surface's separation and bar graphs

The maximum pressure reached in the synovial cavity and the contact area fraction time evolutions along the percentage of the gait cycle %T can be seen in the Fig. 3 together with minimum film thickness during the gait: the maximum pressure follows the trend imposed by the gait vertical load and it increases with respect to the increasing radial clearance; the minimum separation rapidly reaches the zero value due to the direct contact occurring and it seems to reaches this value earlier with a greater radial clearance; the contact area fraction reaches his maximum values during the stance phase (which is the time range going from the 0% to about the 60% of the gait cycle) and it increases its magnitude when the radial clearance decreases, due to the less availability of fluid pressure needed for separate the surfaces.

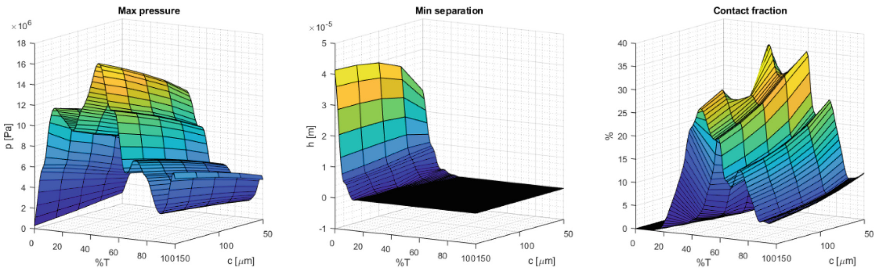

Fig. 3. Maximum pressure, minimum surface separation and contact area fraction evolutions

In the Fig. 4 the components of the eccentricity vector (in its dimensionless form obtained by dividing it by the radial clearance) are reported: even if the *x* component shows a slower decrease with the radial clearance increase, all the components tend to reduce their magnitude when the radial clearance grows and that is due the lower conformity which enhances the availability of pressure within the contact.

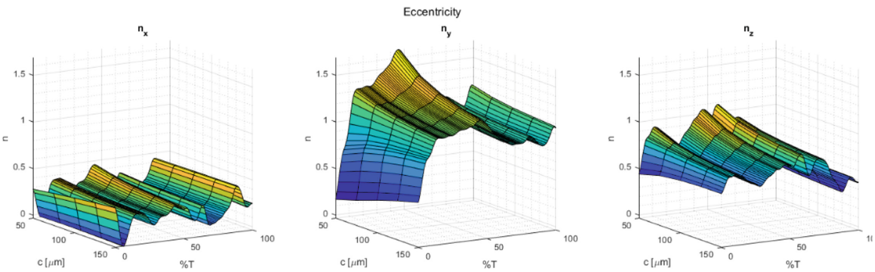

Fig. 4. Eccentricity vector components evolutions

4 Conclusions

A tribological model simulating the mixed lubrication of the artificial hip joint was developed: it is based on the Reynolds equation applied to a discontinuous spherical domain and it is supplied by the hip loads and motion coming from the gait kinematics; it elaborates tribological quantities such as fluid/contact pressure, surface's separation, wear penetration depth and volume, contact fraction area, etc.

The model was used to evaluate the response of the analyzed tribological outputs with respect to an increasing implant radial clearance. The results showed a globally expected trend, which is compliant with the actual decreasing geometrical conformity of the spherical surfaces. A little instability of the contact occurring algorithm arose, suggesting that the principal future investigation has to be devoted to the deepening of other contact occurring approaches; then, other perspectives could regard the introduction of other deformation models based on Finite or Boundary Element approaches, the consideration of the surface roughness with random generators, the study of more sophisticated wear models that take into account the anisotropic mechanical response of the polymeric materials, etc.

References

1. Pramanik, S., Agarwal, A.K., Rai, K.: Chronology of total hip joint replacement and materials development. Trends in Biomater. Artif. Organs **19**(1), 15–26 (2005)
2. Carr, A.J., Robertsson, O., Graves, S., Price, A.J., Arden, N.K., Judge, A., Beard, D.J.: Knee replacement. The Lancet **379**(9823), 1331–1340 (2012); Author, F., Author, S., Author, T.: Book title. 2nd edn. Publisher, Location (1999)
3. Fisher, J., Dowson, D.: Tribology of total artificial joints. Proc. Instit. Mech. Eng. Part H: J. Eng. Med. **205**(2), 73–79 (1991)
4. Zhu, D., Hu, Y.-Z.: The study of transition from elastohydrodynamic to mixed and boundary lubrication. STLE/ASME HS Cheng Tribol. Surveill. 150–156 (1999)
5. Zhu, D.: On some aspects of numerical solutions of thin-film and mixed elastohydrodynamic lubrication. Proc. Inst. Mech. Eng. Part J: J. Eng. Tribol. **221**, 561–579 (2007)
6. Liu, F., Galvin, A., Jin, Z., Fisher, J.: A new formulation for the prediction of polyethylene wear in artificial hip joints. Proc. Instit. Mech. Eng. Part H: J. Eng. Med. **225**(1), 16–24 (2011)
7. Ruggiero, A., Sicilia, A.: A mixed elasto-hydrodynamic lubrication model for wear calculation in artificial hip joints. Lubricants **8**(7), 72 (2020)
8. Ruggiero, A., Sicilia, A.: Musculoskeletal multibody algorithm based on a novel rheonomic constraints definition applied to the lower limb. J. Biomech. Eng. **144**(8), 081010 (2022)
9. Ruggiero, A., Sicilia, A.: Lubrication modeling and wear calculation in artificial hip joint during the gait. Tribol. Int. **142** (2022)
10. Ruggiero, A., Sicilia, A., Affatato, S.: In silico total hip replacement wear testing in the framework of ISO 14242–3 accounting for mixed elasto-hydrodynamic lubrication effects. Wear **460**, 2020 (2020)
11. Ruggiero, A., Sicilia, A.: Mathematical development of a novel discrete hip deformation algorithm for the in silico elasto-hydrodynamic lubrication modelling of total hip replacements. Lubricants **9.4** (2021)
12. Affatato, S., Merola, M., Ruggiero, A.: Development of a novel in silico model to investigate the influence of radial clearance on the acetabular cup contact pressure in hip implants. Materials **11.8** (2018)